RESEARCH PAPER

OncoImmunology 1:5, 593–599; August 2012; © 2012 Landes Bioscience

Sequential metastases of colorectal cancer

Immunophenotypes and spatial distributions of infiltrating immune cells in relation to time and treatments

Sophia Keim,[1,†] Inka Zoernig,[1,†] Anna Spille,[1] Bernd Lahrmann,[2] Karsten Brand,[3] Esther Herpel,[3] Niels Grabe,[2,†] Dirk Jäger[1,†] and Niels Halama[1,†,*]

[1]National Center for Tumor Diseases; Department of Medical Oncology/Internal Medicine VI; University Hospital; Heidelberg, Germany; [2]Tissue Imaging and Analysis Center (TIGA); University Hospital; Heidelberg, Germany; [3]Institute for Pathology, University Hospital; Heidelberg, Germany

[†]These authors contributed equally to this work.

Keywords: colorectal cancer, chemotherapy, immune cell infiltrates, lymphocytes, macrophages

The role of the immune system in the course of colorectal cancer has been elucidated in the last decade. While quantification of immune cell infiltrates within the resected specimen at diagnosis has a clear power to estimate the prognosis of the patient, the role of infiltrating immune cells within the metastatic situation and especially within the metastatic lesion itself requires further detailed analyses. Recent analyses of infiltrates in colorectal cancer liver metastases revealed a role for the infiltrate density not only for prognosis but also in the prediction of treatment response. This not only broadens the view on these infiltrates and indicates a systematic role of the local immunological microenvironment, but also raises the question how these infiltrates change during repeated courses of treatment (i.e., resection, chemotherapy, etc.). To address this question, sequential lung or sequential liver metastases of colorectal cancer patients were analyzed using whole slide image quantification after immunohistochemical staining against CD3, CD8, FOXP3, CD68 and Granzyme B. The clinical data and interventions were associated with each individual patient and the metastatic lesions. The resulting cell densities reveal a heterogeneous profile: after successful treatment of a metastatic lesion, the recurrent lesion can still have the same immunophenotype with similar cell distributions. In a situation of a favorable immune cell profile, this profile can return and apparently convey a similar favorable course throughout the disease. But also the opposite was found: the recurrent metastatic lesion could have a different profile with alterations in specific immune cell subsets over time. Further analyses are required to elucidate the different patterns and their associations to the treatment, the tumor cell phenotype and other dynamic factors. However, it is clear from this data however, that there is an immune cell plasticity that needs to be analyzed for individual patients.

Introduction

The local immune infiltration in colorectal cancer impacts the clinical course of the disease.[1-5] While the vast majority of research focused on the tumor microenvironment in primary colorectal cancer,[6-9] the role of infiltrates becomes now clearer also for the metastatic situation. Recent data show a correlation between the infiltrate density of effector T cells at the metastatic site[10] and the prognosis as well as chemotherapy treatment effectiveness.[11] The composition of the different immune cells and their corresponding cytokines and chemokines shape the local milieu and the subsequent clinical course.[12,13] The intricate interplay between the immune cells present at the tumor site and e.g., chemotherapeutics, radiation or other drugs (i.e., small molecule inhibitors) is being analyzed in great detail.[14-18]

From the clinical perspective, there is an urgent need to improve the medical care of patients with metastatic colorectal cancer. The overall survival for patients with irresectable metastatic disease is still around 24 months, despite the general improvements in the care of this patient cohort.[19,20] A broad array of interventions is used for individual (primarily) irresectable metastatic colorectal cancer patients: chemotherapy (in combination with antibodies), radiation, radio-frequency ablation etc. Using these therapeutic approaches often leads to highly heterogeneous treatment courses between different patients. For example, repeated courses of chemotherapy can lead to a significant shrinkage of the metastatic lesion and subsequent surgical removal. Unfortunately, in many cases, the metastasis recurs after some time and again is treated. Thus, repeated interventions can lead to a series of tissue specimens that are suitable for analysis. For metastases that recur in the same location, it

*Correspondence to: Niels Halama; Email: niels.halama@med.uni-heidelberg.de
Submitted: 03/14/12; Accepted: 03/27/12
http://dx.doi.org/10.4161/onci.20179

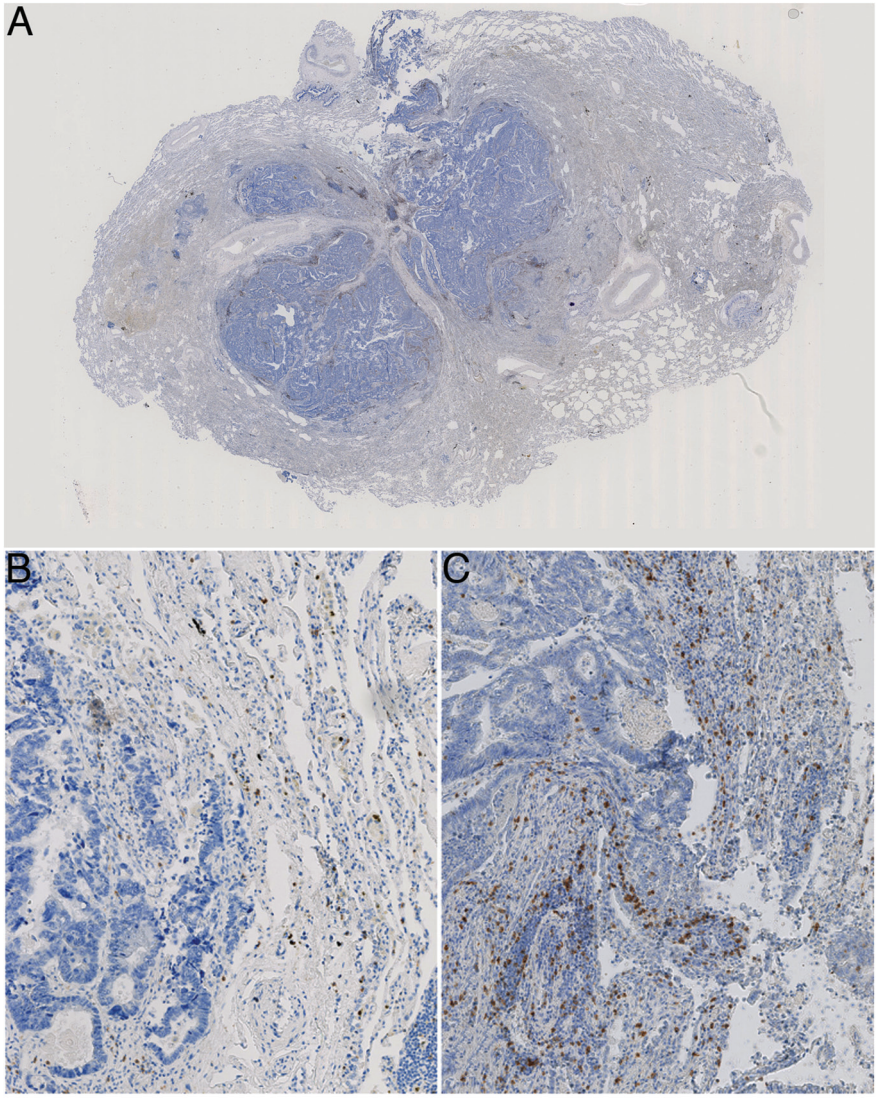

Figure 1. Colorectal cancer lung metastasis. (A) Shows an overview image with the central metastatic site and surrounding normal lung tissue. (B) Shows a 10× magnification of a region within a metastatic lesion with a low density but more homogeneous distribution of stained immune cells ($CD3^+$ cells stained) and (C) shows a more heterogenous distribution of stained immune cells ($CD3^+$ cells stained, distribution skewness near zero).

is most likely that tumor cells from the initial metastasis were left behind as micrometastases. The immune infiltration in these recurrences has not been analyzed systematically, as these recurrences are often not resected or no biopsies are taken. It is entirely unclear, how local (radiofrequency ablation, radiation, etc.) or systemic interventions (chemotherapy, small molecule inhibitors, etc.) effect the local immune cell composition at the metastatic site. As there can be (extended) periods of paused treatment or no treatment, it is also unclear, how stable the immune infiltration is over longer time periods, especially without any medical intervention.

Analyzing these rare tissue specimens of a few selected patients, insights into the impact of local immune cell infiltration on the following clinical course or treatment response can be gained.

The availability of novel technologies to quantify immune cell populations across whole slide sections allows for the first time a reproducible and robust quantification of immune cells. This robustness is necessary to precisely quantify cells in individual patient specimen and thus generate high-resolution data on the spatial heterogeneity and distribution of these cells.[21] Especially effector T cells are seen as the key contributors to the improved clinical outcome in patients with high T cell densities.[22,23] But the role of other immune cell populations, like macrophages or myeloid derived suppressor cells, is not entirely clear. The intricate network of immune cells and the complexities in the interaction between the different cells within the local tumor microenvironment are not well understood.

Here we use whole slide immune cell quantification on tissue specimens from patients with repeated surgical interventions on either lung or liver metastases from colorectal cancer. Using established markers for T cells (CD3, CD8, FOXP3 and Granzyme B), NK cells (NKp46) and macrophages/monocytes (CD68) spatial profiles and densities within the tissue sections were visualized.

Results

Differences in the immune cell subpopulation densities and their distribution were noted across different time points (numbered consecutively on the horizontal axis, for clinical course and tissue specimens see the Patients and Methods section) and in different compartments of the metastatic lesion. For more details on the interpretation of the skewness of cell distributions and associated patterns, please refer to the **Supplemental Material**. As previously identified in reference 11, the invasive margin was analyzed separately and indeed showed distinct patterns, apart from the interior (or center) of the metastasis (**Fig. 1**). **Figure 2A and B** shows the cell densities in the center and in the invasive margin from the lung metastases of patient 1. **Figure 2C and D** show the "skewness" of the distribution of the cell densities across the two different compartments. The icons in **Figure 2A** indicate treatment modalities and in **Figure 2C** the corresponding time points (starting at the first time point of tissue specimen 1 onwards) are shown to indicate the timelines between the three tissue specimens. **Figure 2A** plus **Figure 2C** and **Figure 2B** plus **Figure 2D** thus form the informative basis showing density and distribution of the immune cells in the given compartment.

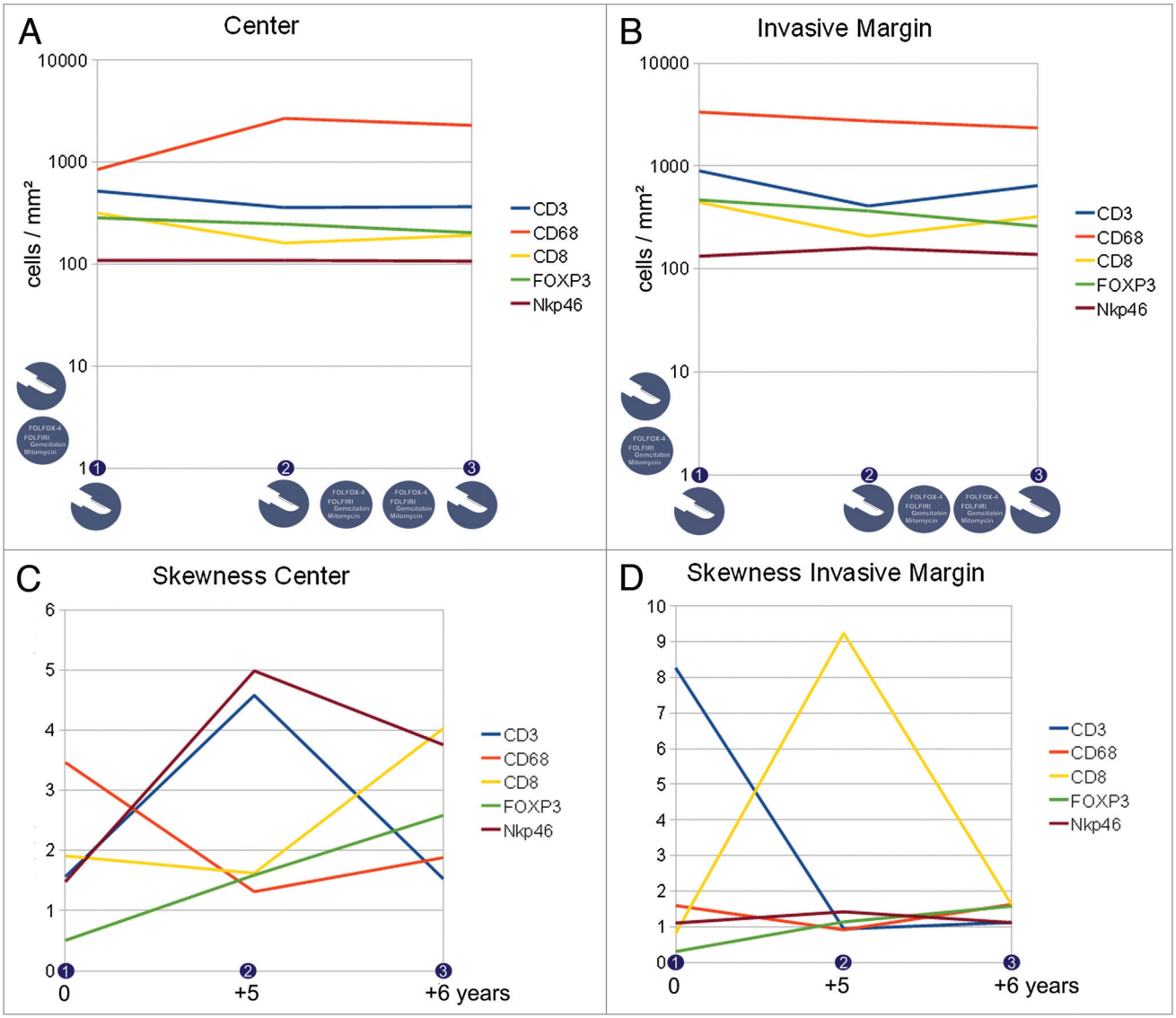

Figure 2. Immune cell densities at the center and the invasive margin of the recurring colorectal cancer lung metastasis (patient 1). (A and B) Cell densities at three different time points (logarithmic scale) and subdivided into center (A) and invasive margin (B), icons indicate treatment modalities (i.e., resection and chemotherapy) at that time point or in between, vertical icons indicate previous treatment modalities. (C and D) Corresponding immune infiltration patterns with a more homogeneous distribution with higher values and a more heterogeneous distribution with values near zero, the time scale corresponds to the time points shown in (A and B) and gives the time from the first tissue specimen.

Figure 3A–D has the same structure and gives the details on the metastatic lesions within the liver of patient 2.

Discussion

Data on patient 1 with lung metastases is presented in **Figure 2**. Cell densities show a clear trend for the CD68 positive cells in the center of the metastatic lesion: these cells increase in number. In the invasive margin, there is a trend toward slightly lower CD68 positive cell numbers. Uniformly, CD8 positive cells show a drop in cell density at time point 2 (tissue specimen 2) in both compartments (center and invasive margin), a phenomenon that is (partly) reversed one year later. CD3 positive cell numbers also drop in density, while FOXP3 positive cells clearly decrease over time. NK cell densities are apparently unchanged during the six years. This is in pronounced contrast to the distribution in the center of the metastasis. NK cells show a flattened distribution pattern (skewness of 5) at time point 2, that contrasts with a near-normal distribution at time point 1 (**Fig. 2C**). This re-distribution was also observed for CD3 positive cells, which in turn is again reversed at time point 3. In contrast, the CD68 positive monocytic/macrophage populations show a change from a "flat" distribution to a more diverse distribution (drop of skewness from 3.5 to 1.5), which is accompanied by a dramatic increase in CD68 positive cell numbers (**Fig. 2A**). In the invasive margin, two main alterations dominate the distributions: CD3 positive cell numbers dramatically shift from a "flat" distribution to a near-normal distribution at time point 2 and 3, whereas the CD8

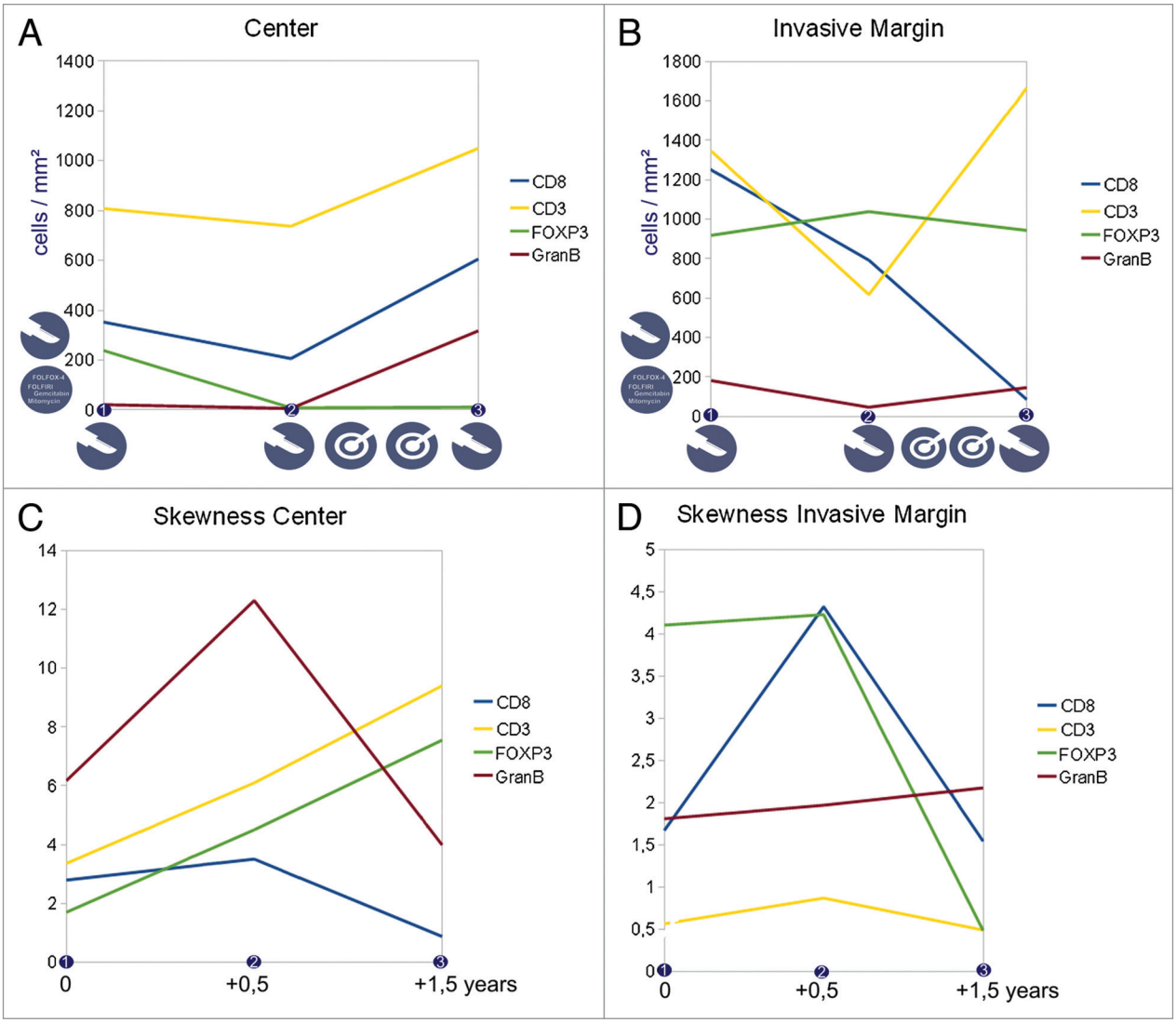

Figure 3. Immune cell densities at the center and the invasive margin of the recurring colorectal cancer liver metastasis (patient 2). (A and B) Cell densities at three different time points (linear scale) and subdivided into center (A) and invasive margin (B), icons indicate treatment modalities (surgical resection and local ablation) at that time point or in between, vertical icons indicate previous treatment modalities (i.e., resection and chemotherapy) (C and D) corresponding immune infiltration patterns with a more homogeneous distribution with higher values and a more heterogeneous distribution with values near zero, the time scale corresponds to the time points shown in (A and B) and gives the time from the first tissue specimen.

positive cells show a "flattening" of the distribution at time point 2 alone, time points 1 and 3 displaying heterogeneous distributions. Chemotherapy was administered between time points 2 and 3, but apparently the cell densities between these time points did not change significantly. FOXP3 positive cells decrease (**Fig. 2A and B**) as well as CD68 positive cells within the invasive margin. In contrast, chemotherapy leads to marked changes in the distribution patterns of CD8 and CD3 positive cells. So the patterns of distribution and not the sheer cell numbers are affected by this treatment. On the other hand, between time points 1 and 2 a significant change of distribution is observed for NKp46, CD8 and CD3 positive cells (**Fig. 2C and D**), without any medical intervention. Presumably, the recurrent cell clone(s) after the resection induced this alteration in immune cell distribution. It is tantalizing to see that the NKp46 positive cell populations did not change dramatically in density across the three time points. However, the distribution patterns at the center of the metastasis flattened out over time and did not reach the initial heterogeneity. CD3 positive cell distributions within the center and at the invasive margin however reached higher heterogeneity (and cluster formation) over time. The processes that dictate T cell and NK cell distributions are apparently diverse, which is in line with earlier observations in primary colorectal cancer and liver metastases.[12] The second interesting observation is, that chemotherapy did not lead to a significantly "lymphocyte depleted" metastatic lesion, but instead the CD3 and CD8 cell numbers increased during chemotherapy, while FOXP3 cell densities decreased. So it is entirely possible, that a "T cell rich" (high density profile) is sustained through chemotherapy and longer time periods.

Data on patient 2 with liver metastasis is presented in **Figure 3**. Some similarities can be found to the observations in patient 1: during periods without medical intervention, the lymphocyte subpopulation densities either are stagnant or decrease within the metastatic site. Interestingly, again the FOXP3 positive cell numbers at the center are declining over time, but at the invasive margin these cells remain constant. Looking at the data before interventional ablation of the other metastases, the distribution pattern for CD8 positive cells again shows a trend toward a "flatter" distribution at the invasive margin, coupled to declining cell numbers. So both metastatic lesions from the two different patients show this phenomenon of lower CD8 positive cell density over time coupled to a more homogeneous distribution (as seen in **Figure 1B**). This seems to be a "natural" development as both patients did not receive any treatment during this phase (time point, 1 to 2). An interesting effect of the radiofrequency-ablation on the cell populations can be observed: densities of CD3, CD8 and Granzyme B positive cells increase at the center of the metastatic lesion for patient 2. At the invasive margin, CD3 and Granzyme B positive cells increase significantly, while CD8 positive cells are further declining. This increased cell density is accompanied by a more heterogeneous cell distribution at the invasive margin. It is noteworthy however, that in the presented case 1, the ablation of other metastatic lesions leads to dramatic alterations at the (analyzed) key metastatic site. The latter was only resected and not treated by local ablation (see Patients and Methods). Of course it cannot be delineated whether the observed changes are inherent of the intervention or if they are dictated by the local tissue parameters (lymphoid structures, etc.). Most likely it is a combination of both.

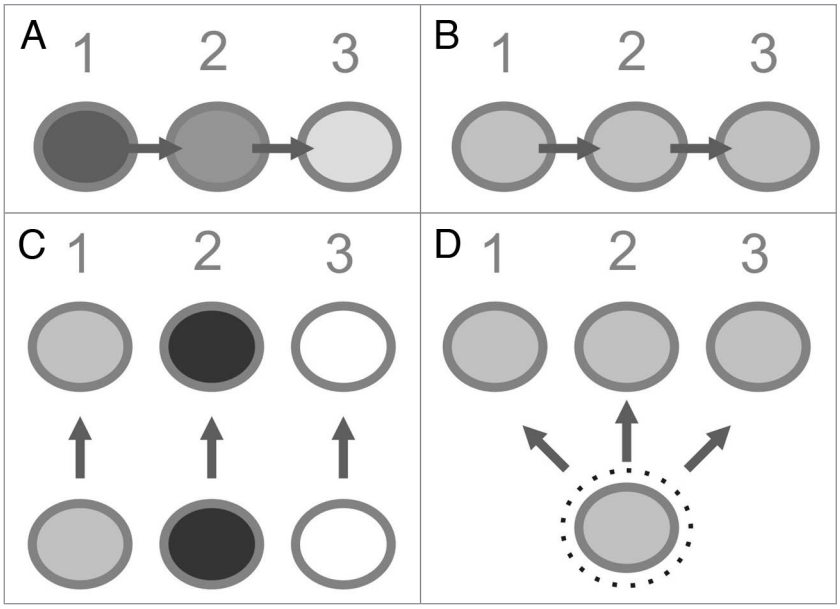

Figure 4. Some (theoretical) immune cell patterns across repeated resections and treatments (time points 1–3) and the hypothetical founding tumor cell(s). Shading of circles indicates T cell density (light: low density-black: high density). (A) Shows the sequence estimated from clonal selection: the initial T cell rich phenotype disappears over time and the chemotherapy-resistant tumor cells recur. (B) Depicts the sequence as also observed in this work, showing a consistent immune cell pattern over time and after treatments (with repopulation occurring from the same metastatic site). (C) Is assuming that the metastatic site is re-populated by different tumor cells from different other tumor sites, inducing distinct microenvironmental conditions. (D) Shows the hypothetical explanation for a consistent immunologic phenotype over time as there is a "protected environment" for the founding tumor cell where chemotherapy cannot induce a selection.

In a similar direction, it cannot be clarified from which cell population the metastatic lesion was recurring after the surgical interventions. As mouse data shows, the migration from tumor cells between different sites can occur[24] and in advanced cancer stages, micrometastasis has likely happened. The phenotype of the immune cells however can be used to assess some of the possibilities. **Figure 4** shows some considerations to the observed immune cell patterns across time and treatments.

Looking at the data and comparing the identified thresholds[11] for both metastatic lesions over time, it is clear that after successful treatment of a metastatic lesion, the recurrent lesion can (A) still have the same immunophenotype with similar cell distributions or (B) regain the initial phenotype. The immunophenotype in these cases can either be indicative of good prognosis or treatment response or also indicative of the opposite, i.e., worse prognosis and treatment failure. In a situation of a favorable immune cell profile, this profile can return and apparently convey a similar favorable course throughout the disease (**Fig. 4B**). But also the opposite was found: the recurrent metastatic lesion could have a different profile with significant alterations in specific immune cell subsets (**Fig. 4A or C**). So further work is needed to understand what intervention or mechanisms trigger either the change in the local immune profile or lead to a stable consistent profile over time and treatments. The multitude of parameters involved in this makes it difficult to draw easy conclusions but only systematic analyses of serial tissue specimens can yield enough information to deduce key factors.

In summary, the presented data shows that the plasticity of the immune infiltration is high and processes fueled by the heterogeneity of the tumor cell subpopulations as well as immunologic changes drive the alterations in the local immune profile. Combining the specifics and effects of different interventions, i.e., chemotherapy vs. ablation, adds to this complexity and requires further analyses of the underlying dynamics.

Patients and Methods

Tissue was obtained from the Surgical Department of the University Hospital in Heidelberg and serial sections for immunohistochemistry were prepared by the tissue bank of the NCT Heidelberg.

Patient 1 with lung metastases. The patient was diagnosed with colorectal cancer, which was resected completely and

adjuvant chemotherapy was given. Four years later the patient developed lung metastases that were removed surgically (tissue specimen 1). Again, five years later lung metastases occurred and a partial resection was performed (tissue specimen 2). Chemotherapy was started using FOLFOX-6, which was successful in reducing the metastatic burden significantly, but had to be terminated due to side effects. After a pause, chemotherapy was continued with FOLFIRI. Due to the repeated decrease in metastatic burden, resection of the lung metastasis was performed (tissue specimen 3). Beyond this time point, the patient has received multiple different chemotherapies and antibodies in different combinations (cetuximab, bevacizumab, panitumumab, capecitabine, irinotecan, FOLFOX and FOLFIRINOX) and responded to these treatments during a timeframe of seven years. The patient is still alive, 18 y after the diagnosis of colorectal cancer. The precise TNM classification of the initial primary colorectal cancer was not available, whereas the histological workup clearly documented colorectal cancer of the sigma.

Patient 2 with liver metastases. This patient was diagnosed with colorectal cancer with synchronous liver metastasis (pT3, N2, M1, G2) and the complete tumor burden in the colon and the liver was resected. Afterwards the patient received adjuvant chemotherapy, but approximately half a year later recurrent liver metastasis was noted. After resection of the recurrent metastasis (tissue specimen 1), five months later another recurrence within the liver was diagnosed and removed (tissue specimen 2). In another part of the liver, new metastases occurred and were treated with radiofrequency-ablation. A year later, another recurrence in the initial site occurred and was surgically removed (tissue specimen 3). Another year later, new irresectable metastases occurred and palliative chemotherapy was initiated. The patient then received multiple different chemotherapies and antibodies (FOLFOX, FOLFIRI, capecitabine, bevacizumab and Cetuximab). 60 months after initial diagnosis best supportive care was started as the clinical situation worsened dramatically. Unfortunately, no further information is available.

Immunohistochemical staining. Tissue specimens were immunohistochemically analyzed for their infiltration with CD3, CD8, Granzyme B, FOXP3, NKp46 and CD68 positive immune cells. Tissue sections (4 μm) were prepared from formalin-fixed, paraffin-embedded tissue. After deparaffinization and rehydration, the slides were transferred to a fully automated staining facility (Leica BOND-MAX™, Leica Microsystems) to optimize the comparability. The slides were boiled in 10 mM citrate buffer (pH 6) for 20 min to retrieve the antigens. For NKp46 stains, slides were incubated with proteinase K at 37.5°C for 5 min instead. The endogenous peroxidase activity was blocked by incubation with 0.6% H_2O_2 in methanol for 10 min. The sections were blocked with 10% normal goat serum (Vectastain® Elite ABC kit, Vector). Mouse monoclonal antibodies recognizing human CD3ε (1:50 dilution, clone PS1, Acris), CD8 (1:40 dilution, clone 4B11, Novocastra), GrB (1:50 dilution, clone 11F1, Novocastra), FOXP3 (1:100 dilution, clone 236A/E7, Abcam), NKp46 (1:175 dilution, clone 195314, R&D Systems) and CD68 (1:200 dilution, clone KP1, Abcam) were applied as primary antibodies at room temperature for 30 min. The slides were incubated with a secondary antibody (rabbit-anti-mouse IgG, Bond Refine Detection Kit, Leica) for 8 min at room temperature. Further amplification of the signal was achieved through incubation with a third antibody, conjugated with horse radish peroxidase and coupled to dextrane molecules in large numbers, for 8 min at room temperature (mouse-anti-rabbit IgG, Bond Refine Detection Kit, Leica). The antigen detection was performed by a color reaction with 3,3-diamino-benzidine (DAB^+ chromogen, Leica). The sections were counterstained with hematoxylin (Leica) and mounted with Aquatex (Merck).

Evaluation of immunohistochemical variables. The number of stained immune cells was counted using a computerized image analysis system consisting of a NDP Nanozoomer from Hamamatsu Photonics attached to a personal computer. Complete microscopic images of full tissue sections were automatically obtained for later automatic or visual analysis (virtual microscopy), allowing large scale histological evaluation with high precision across the complete section. Thus, varying cell densities across the complete tissue section can be measured objectively. In this analysis, the average cell density across the measured region was used as well as the individual density of cells for each 1 mm^2 of tissue analyzed. The "invasive margin" was defined as a region of 500 μm width on each side of the border between malignant cells ("metastasis" and peritumoral stroma) and liver or lung tissue (see supporting information in **Fig. 1**). The remaining part of the metastasis was termed "center" and analyzed separately.

The results were expressed as the mean of positive stained cells per mm^2. A total of 367,727 mm^2 of tissue surface area was analyzed. Cell counts were assessed with a specifically developed software program (VIS software suite, Visiopharm) to measure cell densities across a given region of interest as reported previously in references 11, 21 and 25. All evaluations were visually checked for consistency.

Statistical analysis. To estimate complexity of the spatial patterns, the "skewness" (v) of the distribution of the cell counts for individual 1 mm^2 fields was used. **Supplemental Table 1 and Supplemental Figure 1** show some examples of the obtained values for v and corresponding exemplary distributions of cell densities across a tissue. The definition of the skewness of a distribution can be found in the **Supplemental Material** and was computed with SPSS 19.0 (IBM).

Disclosure of Potential Conflicts of Interest

No potential conflicts of interest were disclosed.

Supplemental Material

Supplemental materials may be found here:
www.landesbioscience.com/journals/oncoimmunology/article/20179

References

1. Galon J, Costes A, Sanchez-Cabo F, Kirilovsky A, Mlecnik B, Lagorce-Pagès C, et al. Type, density and location of immune cells within human colorectal tumors predict clinical outcome. Science 2006; 313:1960-4; PMID:17008531; http://dx.doi.org/10.1126/science.1129139.
2. Bindea G, Mlecnik B, Fridman WH, Pagès F, Galon J. Natural immunity to cancer in humans. Curr Opin Immunol 2010; 22:215-22; PMID:20207124; http://dx.doi.org/10.1016/j.coi.2010.02.006.
3. Pagès F, Berger A, Camus M, Sanchez-Cabo F, Costes A, Molidor R, et al. Effector memory T cells, early metastasis and survival in colorectal cancer. N Engl J Med 2005; 353:2654-66; PMID:16371631; http://dx.doi.org/10.1056/NEJMoa051424.
4. Pagès F, Galon J, Dieu-Nosjean MC, Tartour E, Sautès-Fridman C, Fridman WH. Immune infiltration in human tumors: a prognostic factor that should not be ignored. Oncogene 2010; 29:1093-102; PMID:19946335; http://dx.doi.org/10.1038/onc.2009.416.
5. Pagès F, Kirilovsky A, Mlecnik B, Asslaber M, Tosolini M, Bindea G, et al. In situ cytotoxic and memory T cells predict outcome in patients with early-stage colorectal cancer. J Clin Oncol 2009; 27:5944-51; PMID:19858404; http://dx.doi.org/10.1200/JCO.2008.19.6147.
6. Deschoolmeester V, Baay M, Van Marck E, Weyler J, Vermeulen P, Lardon F, et al. Tumor infiltrating lymphocytes: an intriguing player in the survival of colorectal cancer patients. BMC Immunol 2010; 11:19; PMID:20385003; http://dx.doi.org/10.1186/1471-2172-11-9.
7. Diederichsen ACP, Hjelmborg JB, Christensen PB, Zeuthen J, Fenger C. Prognostic value of the $CD4^+$/$CD8^+$ ratio of tumour infiltrating lymphocytes in colorectal cancer and HLA-DR expression on tumour cells. Cancer Immunol Immunother 2003; 52:423-8; PMID:12695859; http://dx.doi.org/10.1007/s00262-003-0388-5.
8. Prall F, Dührkop T, Weirich V, Ostwald C, Lenz P, Nizze H, et al. Prognostic role of $CD8^+$ tumor-infiltrating lymphocytes in stage III colorectal cancer with and without microsatellite instability. Hum Pathol 2004; 35:808-16; PMID:15257543; http://dx.doi.org/10.1016/j.humpath.2004.01.022.
9. Ohtani H. Focus on TILs: prognostic significance of tumor infiltrating lymphocytes in human colorectal cancer. Cancer Immun 2007; 7:4; PMID:17311363.
10. Halama N, Michel S, Kloor M, Zoernig I, Pommerencke T, von Knebel Doeberitz M, et al. The localization and density of immune cells in primary tumors of human metastatic colorectal cancer shows an association with response to chemotherapy. Cancer Immun 2009; 9:1; PMID:19226101.
11. Halama N, Michel S, Kloor M, Zoernig I, Benner A, Spille A, et al. Localization and density of immune cells in the invasive margin of human colorectal cancer liver metastases are prognostic for response to chemotherapy. Cancer Res 2011; 71:5670-7; PMID:21846824; http://dx.doi.org/10.1158/0008-5472.CAN-11-0268.
12. Halama N, Braun M, Kahlert C, Spille A, Quack C, Rahbari N, et al. Natural killer cells are scarce in colorectal carcinoma tissue despite high levels of chemokines and cytokines. Clin Cancer Res 2011; 17:678-89; PMID:21325295; http://dx.doi.org/10.1158/1078-0432.CCR-10-2173.
13. Mlecnik B, Tosolini M, Charoentong P, Kirilovsky A, Bindea G, Berger A, et al. Biomolecular network reconstruction identifies T-cell homing factors associated with survival in colorectal cancer. Gastroenterology 2010; 138:1429-40; PMID:19909745; http://dx.doi.org/10.1053/j.gastro.2009.10.057.
14. Apetoh L, Tesniere A, Ghiringhelli F, Kroemer G, Zitvogel L. Molecular interactions between dying tumor cells and the innate immune system determine the efficacy of conventional anticancer therapies. Cancer Res 2008; 68:4026-30; PMID:18519658; http://dx.doi.org/10.1158/0008-5472.CAN-08-0427.
15. Casares N, Pequignot MO, Tesniere A, Ghiringhelli F, Roux S, Chaput N, et al. Caspase-dependent immunogenicity of doxorubicin-induced tumor cell death. J Exp Med 2005; 202:1691-701; PMID:16365148; http://dx.doi.org/10.1084/jem.20050915.
16. Zitvogel L, Apetoh L, Ghiringhelli F, André F, Tesniere A, Kroemer G. The anticancer immune response: indispensable for therapeutic success? J Clin Invest 2008; 118:1991-2001; PMID:18523649; http://dx.doi.org/10.1172/JCI35180.
17. Zitvogel L, Kepp O, Aymeric L, Ma Y, Locher C, Delahaye NF, et al. Integration of host-related signatures with cancer cell-derived predictors for the optimal management of anticancer chemotherapy. Cancer Res 2010; 70:9538-43; PMID:21098713; http://dx.doi.org/10.1158/0008-5472.CAN-10-1003.
18. Zitvogel L, Kepp O, Kroemer G. Immune parameters affecting the efficacy of chemotherapeutic regimens. Nat Rev Clin Oncol 2011; 8:151-60; PMID:21364688; http://dx.doi.org/10.1038/nrclinonc.2010.223.
19. Jemal A, Siegel R, Ward E, Murray T, Xu J, Smigal C, et al. Cancer statistics. CA Cancer J Clin 2006; 56:106-30; PMID:16514137; http://dx.doi.org/10.3322/canjclin.56.2.106.
20. Kopetz S, Chang GJ, Overman MJ, Eng C, Sargent DJ, Larson DW, et al. Improved survival in metastatic colorectal cancer is associated with adoption of hepatic resection and improved chemotherapy. J Clin Oncol 2009; 27:3677-83; PMID:19470929; http://dx.doi.org/10.1200/JCO.2008.20.5278.
21. Halama N, Zoernig I, Spille A, Michel S, Kloor M, Grauling-Halama S, et al. Quantification of prognostic immune cell markers in colorectal cancer using whole slide imaging tumor maps. Anal Quant Cytol Histol 2010; 32:333-40; PMID:21456345.
22. Halama N, Zoernig I, Grabe N, Jaeger D. The local immunological microenvironment in colorectal cancer as a prognostic factor for treatment decisions in the clinic: The way ahead. OncoImmunology 2012; 1:62-6; http://dx.doi.org/10.4161/onci.1.1.18460.
23. Tosolini M, Kirilovsky A, Mlecnik B, Fredriksen T, Mauger S, Bindea G, et al. Clinical impact of different classes of infiltrating T cytotoxic and helper cells (Th1, th2, treg, th17) in patients with colorectal cancer. Cancer Res 2011; 71:1263-71; PMID:21303976; http://dx.doi.org/10.1158/0008-5472.CAN-10-2907.
24. Kim MY, Oskarsson T, Acharyya S, Nguyen DX, Zhang XH, Norton L, et al. Tumor self-seeding by circulating cancer cells. Cell 2009; 139:1315-26; PMID:20064377; http://dx.doi.org/10.1016/j.cell.2009.11.025.
25. Halama N, Zoernig I, Spille A, Westphal K, Schirmacher P, Jaeger D, et al. Estimation of immune cell densities in immune cell conglomerates: an approach for high-throughput quantification. PLoS One 2009; 4:7847; PMID:19924291; http://dx.doi.org/10.1371/journal.pone.0007847.